International Journal of Thermophysics, Vol. 11, No. 2, 1990

Present Research on Thermal Radiation Properties and Characteristics of Materials[1]

T. Makino[2]

This paper reviews the recent advances in our spectroscopic research on radiation properties and characteristics of solid and liquid materials, from thermal engineering point of view. The topics discussed are optical constants of metallic materials, radiation characteristics of the real surfaces in actual industrial environments, those of semi-transparent scattering-absorbing media, and those of human body and environmental surfaces of human living space. The review also includes the algorithm for radiation pyrometry and the demand for radiation data of new materials and for new engineering techniques. It is concluded that the development of engineering models is important for the systematic research of the complicated radiation phenomena and that generation and compilation of pertinent data are necessary.

KEY WORDS: emittance; metallic materials; optical constants; radiation properties; radiation pyrometry; reflectance; scattering-absorbing medium; thermal radiation.

1. INTRODUCTION

The demand for the knowledge on thermal radiation properties and characteristics of materials is increasing for new and/or greater industrial production and also for the improvement in the human life-style, related to thermal engineering designs and also to thermal measurement techniques. In spite of the increasing demand, a satisfactory systematic method for the research of thermal radiation phenomenon has not yet been established. The thermal radiation phenomenon is complicated and depends strongly on conditions of the material and the surface. The present paper discusses some of the topics related to the above problems.

[1] Paper presented at the Second U.S.–Japan Joint Seminar on Thermophysical Properties, June 23, 1988, Gaithersburg, Maryland, U.S.A.

[2] Department of Engineering Science, Kyoto University, Kyoto 606, Japan.

0195-928X/90/0300-0339$06.00/0

2. OPTICAL CONSTANTS OF METALS AND ALLOYS

The thermal radiation phenomenon for metallic materials is characterized by two factors: the electronic properties of the materials, which are represented by the optical constants, and the surface conditions, which are microscopic roughness, oxide film, and contaminations. We begin the discussion with the topics on the optical constants.

The electronic properties are important as a basis of the characteristics of real surfaces, since the effects of the surface conditions are not independent of the properties. Also, when the characteristics of real surfaces are so complicated that the most probable values may not be evaluated, the optical constants offer the knowledge of the minimum radiation transfer possible. For the thermal engineering applications, the constants should be obtained over wide spectral and temperature regions, and it is preferable to correlate the constants as functions of wavelength and temperature.

We proposed a method for the need [1]. A basic formula of optical constant dispersion is adopted. The equation has the same form as the Drude-Roberts' equation [2]. The dispersion of the optical constant $\hat{n} = n - ik$ is described by

$$\hat{n}^2 = 1 + \frac{S\lambda^2}{\lambda^2 - \lambda_0^2 + i\delta\lambda_0\lambda} - \frac{\lambda^2}{2\pi c\varepsilon_0} \sum_{k=1}^{2} \frac{\sigma_k}{\lambda_k - i\lambda} \tag{1}$$

where λ is the wavelength of radiation in vacuum, the unity (the first term on the right-hand side) is the relative dielectric constant of vacuum, and the following two terms represent the contributions of the interband and intraband (conduction absorption) transitions of electrons in a classical model. The symbols S, λ_0, and δ are the strength, central wavelength, and parameter for damping, respectively; σ_k and λ_k, the kth ($k = 1, 2$) component of d.c. (direct current) electrical conductivity and relaxation wavelength for σ_k, respectively; c, speed of radiation in vacuum; and ε_0, (absolute) dielectric constant of vacuum. First, spectra of reflectivity and/or emissivity are measured. Second, the qualitative tendencies of the spectra are diagnosed to choose the dominant terms in Eq. (1). The other terms are abbreviated for the decisive analysis. Third, the spectra are analyzed at each temperature to determine the values of the electronic parameters in the simplified formula. Finally, the temperature dependence of the parameters are investigated theoretically or empirically to correlate them in the form of equations. Such equations are written as follows:

$$\sigma_0 = \sigma_1 + \sigma_2 = 1 \Big/ \left(\sum_{l=0}^{3} a_l T^l \right) \tag{2}$$

and

$$\partial(S, \lambda_0, \delta, \sigma_1/\lambda_1, \sigma_2/\lambda_2, \sigma_2)/\partial T = 0 \tag{3}$$

where T is the temperature. Equation (3) means that these quantities are independent of T. An example of the simplified form of Eq. (1) is

$$\hat{n}^2 = 1 + (S - iS\,\delta\lambda_0/\lambda) - \frac{\lambda^2}{2\pi c\varepsilon_0} \sum_{k=1}^{2} \frac{\sigma_k}{\lambda_k - i\lambda} \tag{4}$$

This equation may be used for molten metals. The temperature dependence of $(S\,\delta\lambda_0)$ is written by

$$S\,\delta\lambda_0 = \sum_{m=0}^{1} b_m T^m \tag{5}$$

This method has been applied to the study on the properties of many metallic materials: carbon steels [3, 4], heat-resisting alloys [5], their constituent transition metals [3, 4, 6], and refractory metals [7]. It has also been applied to some metals and alloys in the liquid state [8] and to that of electrically conducting ceramics [7]. Table I summarizes the results [1], where the unit S is "siemens" in the SI units. The values in the table are readily used in Eqs. (1)–(3) or in Eqs. (3)–(5). The optical constants are calculated systematically as functions of wavelength and temperature. We recommend the above method for thermal engineering applications. In the course of these works interesting remarks were obtained: the carbon steels may be recognized as irons including a small amount of impurity [3, 4], while the heat-resisting alloys have similar properties despite their different chemical compositions. The thermal radiation properties of the heat-resisting alloys have particularly close relationship with their electrical conductivities [5]. A clear hysteresis phenomenon is observed in the emissivity of cobalt, which is caused by the martensite transformation and the relaxation of the residual strain [6]. During melting of nickel, a clear increase in the emissivity is observed [8]. Figures 1a and 1b show the two transition phenomena, where ε_N is the normal emissivity. These phenomena are interesting in metallurgical and metrological applications.

3. METALLIC MATERIALS IN INDUSTRIAL ENVIRONMENTS

Radiation characteristics of metallic materials of the real surfaces are characterized mainly by the surface roughness and the surface film and the changes of the conditions in the actual industrial environments. The values

Table I. Dispersion Parameters of Optical Constants of Metallic Materials

	T (K)	S	λ_0 (m $\times 10^{-6}$)	δ	$S\delta\lambda_0$ (m $\times 10^{-6}$)	a_0 ($\Omega \cdot$ m $\times 10^{-7}$)	a_1 ($\Omega \cdot m \cdot K^{-1}$ $\times 10^{-10}$)	a_2 ($\Omega \cdot m \cdot K^{-2}$ $\times 10^{-13}$)	a_3 ($\Omega \cdot m \cdot K^{-3}$ $\times 10^{-17}$)	σ_1/λ_1 ($S \cdot m^{-2}$ $\times 10^{11}$)	σ_2/λ_2 ($S \cdot m^{-2}$ $\times 10^{12}$)	σ_2 ($S \cdot m^{-1}$ $\times 10^{6}$)
Iron (99.96%)												
α, ferro.	200–1043	0				0	0.949	8.70		1.23	2.94	0.45
α, ferro.	800–1043	0				0	1.92	8.21		1.20	1.41	0.47
α, para.	1043–1185	0				0.690	9.82			1.20	1.41	0.47
γ	1185–1600	0				8.81	2.97			1.20	1.41	0.47
Liquid	1700–1900	2.12				18.1	1.80			4.85		0
						$(b_0 = -7.90 \times 10^{-5}$ m, $b_1 = 5.66 \times 10^{-8}$ m $\cdot$ K$^{-1})$						
Cobalt (99.9%)												
hcp, buffed	250–500	57.7	1.46	1.38		2.56	−5.42	12.8		1.53	($\lambda_2 = 0$ m)	0.27
hcp, annealed	250–500	57.7	1.46	1.38		2.17	−5.42	12.8		1.75	($\lambda_2 = 0$ m)	0.27
fcc	800–1400	0				−3.01	10.2	0.0627		1.11	1.13	0.51
Nickel (99.97%)												
Ferro.	250–631	0				1.87	−6.23	15.2		2.23	2.42	0.77
Para.	631–1700	0				2.93	2.92			2.23	2.42	0.77
Liquid	1500–1900	0				8.33	0.96			($\lambda_1 = 0$ m)		0
Chromium (99.8%)	280–1000	37.1	0.82	1.70		5.79	−9.88	17.4		1.87	($\lambda_2 = 0$ m)	0.18
Mild steel (SS41)												
α, ferro.	200–1043	0				0.166	2.52	8.70		1.23	2.94	0.45
α, ferro.	800–1043	0				0.594	1.92	8.21		1.20	1.41	0.47
α, para.	1043–1135	0				−11.3	21.8			1.20	1.41	0.47
γ	1135–1600	0				10.11	2.97			1.20	1.41	0.47
Hard steel (S55C)												
α, ferro.	200–1043	0				0.0643	3.70	8.70		1.23	2.94	0.45
α, ferro.	800–1043	0				3.05	1.92	8.21		1.20	1.41	0.47
γ	1043–1600	0				10.89	2.97			1.20	1.41	0.47
Liquid	1750–1900	7.86				19.1	1.80			4.85		0
						$(b_0 = -7.90 \times 10^{-5}$ m, $b_1 = 5.66 \times 10^{-8}$ m $\cdot$ K$^{-1})$						

Cast iron (3.4%C)										
Liquid	1400–1900	4.80		21.9	1.80			4.85		0
			$(b_0 = -7.90 \times 10^{-5}\ \mathrm{m},\ b_1 = 5.66 \times 10^{-8}\ \mathrm{m \cdot K^{-1}})$							
JIS SUS 304										
	200–600	0		8.17	8.00			0.871	0.864	0.49
	600–1600	0		7.96	10.7	−4.33	6.68	0.871	0.864	0.49
Liquid	1700–1900	1.29		15.0	2.81			8.55		0
			$(b_0 = -1.15 \times 10^{-5}\ \mathrm{m},\ b_1 = 1.55 \times 10^{-8}\ \mathrm{m \cdot K^{-1}})$							
JIS SUS 316	200–600	0		7.89	7.46			0.804	0.890	0.50
	600–1600	0		7.44	11.0	−5.36	10.9	0.804	0.890	0.50
Incoloy 800	200–600	0		9.14	4.86			0.689	1.12	0.60
	600–1600	0		8.62	8.12	−4.72	12.4	0.689	1.12	0.60
X-40 (Stellite 31)	200–600	0		9.03	3.79			3.62	1.65	0.46
	600–1600	0		7.06	10.9	−7.71	21.8	3.62	1.65	0.46
Hastelloy X	200–870	0		12.99	2.29			3.53	0.696	0.22
	870–1600	0		15.37	−1.17	0.655	1.15	3.53	0.696	0.22
Inconel 600	200–750	0		11.04	1.45			3.21	0.628	0.15
	750–1600	0		14.78	−6.79	5.21	−10.5	3.21	0.628	0.15
Inconel 617	200–860	0		13.38	1.65			3.47	0.565	0.14
	860–1600	0		19.05	−9.12	5.94		3.47	0.565	0.14
Molybdenum (99.97%)	290–1400	19.5	12.9	0.588	3.51			5.66	$(\lambda_2 = 0\ \mathrm{m})$	0.218
Tantalum (99.99%)	290–1300	6.51	3.22	−0.190	9.47			4.06	$(\lambda_2 = 0\ \mathrm{m})$	0.107
Tungsten (99.99%)	290–1400	6.44	3.47	1.77	3.63			2.27	$(\lambda_2 = 0\ \mathrm{m})$	0.206
Titanium carbide										
Sintered	294	7.85	3.59	$(\sigma_0 = 1.82 \times 10^6\ \mathrm{S \cdot m^{-1}})$				1.15	$(\lambda_2 = 0\ \mathrm{m})$	0.252
CVD	290–1400	8.45	2.90	0.464	15.4			0.990	$(\lambda_2 = 0\ \mathrm{m})$	0.299
Titanium nitride										
Sintered	292	5.12	0.514	$(\sigma_0 = 1.92 \times 10^6\ \mathrm{S \cdot m^{-1}})$				0.698	0.452	0.656
CVD	290–1200	8.13	0.783	0.842	7.24			1.04	0.568	0.972

of the thermal radiation properties reported in the data books show great scatter [9]. We recently proposed high-speed spectroscopy as an experimental method for investigating radiation characteristics of materials [10, 11]. The high-speed spectrophotometer measures spectra of specular and/or diffuse reflectance in the visible to infrared region repeatedly with a period of less than 1 s. The radiation phenomenon is investigated not by a term of a property value, but as a transition phenomenon of radiation spectrum. Figure 2 is an example of the measured results [10], which shows the behavior of the near-normally (12°) incident specular reflectance of copper (specular-finished surface) in an air-oxidation process at high temperatures. The reflectance R^*_{NN} is a normalized one by the value of the reflectivity R_{NN}(Standard) of the original specular-finished surface, t is the

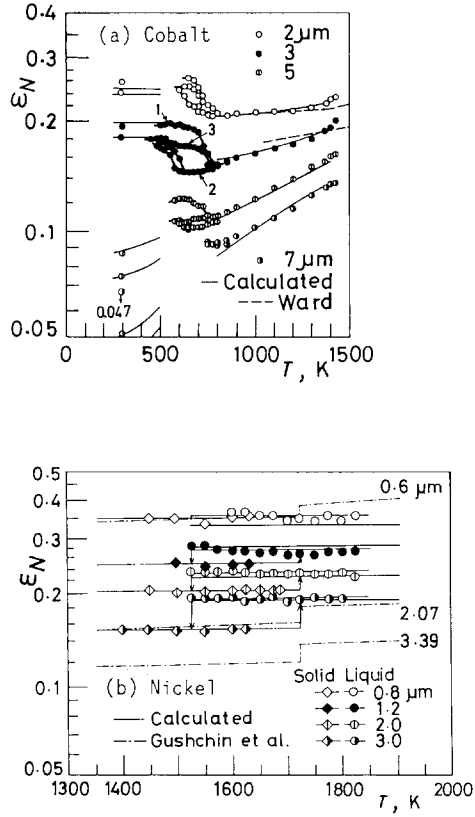

Fig. 1. (a) Behavior of emissivity of cobalt around the phase transition temperature; (b) behavior of emissivity of nickel around the melting temperature.

time after the start of heating, and d is the oxide film thickness evaluated from the results. With the growth of the oxide film, clear interference of radiation is observed. The phenomenon is caused by two factors: the interference at the upper and lower boundaries of the film and the diffraction of radiation at the micro-roughness of the crystal grains of the polycrystalline oxide. Similar interference has been observed also in the diffuse reflectance spectra of oxidizing specular- and rough-finished surfaces. This phenomenon has been reproduced well in many metallic materials [12]. It suggests the possibility of the theoretical modelling of radiation phenomenon of the real surfaces.

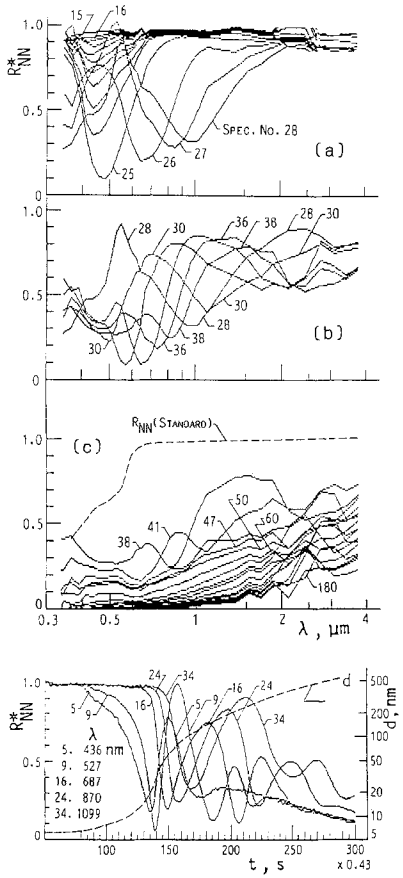

Fig. 2. Transition in R^*_{NN}. spectrum of copper (specular-finished surface) in an air-oxidation process at high temperatures.

The surface model should be a three-dimensional one for the hemispherical flux estimation in the thermal engineering applications. The statistical model of the roughness is desirable to be of a multi-dispersion type [13]. For the surface film, a three-dimensionally non-parallel film element model has been proposed to describe the phenomenon at a poly-crystalline grain of the oxide film [14]. The interference and diffraction of electromagnetic radiation are investigated on a basis of the Kirchhoff's diffraction theory.

Surfaces in cryogenic vacuum systems are comparatively clean and stable, but they sometimes suffer from the deposition of residual gases in the system, which increases the emittance of the surface significantly. Figure 3 shows the spectra of optical constants of an air-cryodeposit film at 20 K [15], where P_{H_2O} is the partial pressure of water in the artificial air

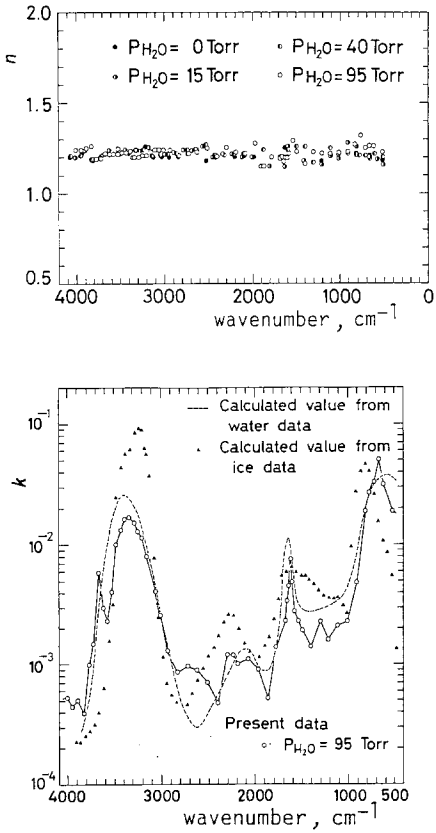

Fig. 3. Spectra of optical constants of an air-cryodeposit film.

with the standard content of carbon dioxide. The properties are correlated by a similar method as that mentioned in Section 2. Further investigations are desirable for the effects of surface roughness and the non-parallel film formation [14] and also for the characteristics of the frost-type deposition.

4. SEMITRANSPARENT SCATTERING-ABSORBING MEDIA

Some materials in thermal engineering applications are semi-transparent scattering-absorbing media for radiation such as paint layers [16], ceramics [17], fibrous insulation materials [18], and polymer gels for a solar pond [19]. The radiation transfer equation describes the phenomenon, provided the spectral and angular characteristics are known exactly. But most of these materials have various chemical compositions and/or physical structures, and they have strong spectral dependence. Most of numerical calculations have dealt the angular characteristics of scattering in detail, but they have neglected the strong spectral characteristics with the gray approximation. On the other hand, we have chosen in our spectral and experimental works a crude approximation of a flux model for the angular characteristics. In order to demonstrate our idea, we show a simple numerical experiment and evaluate the prediction of the flux model.

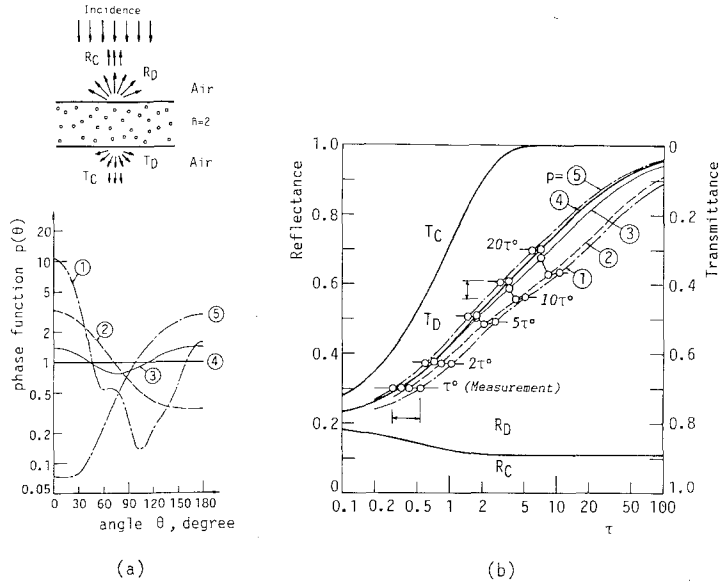

Fig. 4. (a) Scattering layer and presumed phase functions; (b) influences of the choice of phase function on τ and T_H.

Consider a scattering non-absorbing layer of thickness d is irradiated normally by a collimated flux, as shown in Fig. 4a. Notations T and R stand for the transmittance and reflectance, respectively, and subscripts H, C, and D for the hemispherical, collimated, and diffuse components, respectively. The transmittance T_H $(=T_C+T_D)$ of this system is measured to obtain the extinction coefficient K_e. The purpose of the research is the evaluation of the macroscopic values, such as T_H of a similar layer with different d. First, we prepare various kinds of phase functions $p(\theta)$, which are shown in Fig. 4a by the symbols ① ~ ⑤. By using these phase functions, we calculate the behavior of T_C, T_D, R_C, and R_D with the optical thickness τ $(=K_e \cdot d)$. Exact solution of the radiation transfer equation is used at this stage. Figure 4b shows the results. Then we analyze the results, which are the experimental values. Here we arbitarily choose one phase function of the five functions ① ~ ⑤ and believe it to be the "true" function. The experimental value of T_H in the figure corresponds to a unique value of τ^0(Measurement), which determines K_e by τ^0/d. As seen in the

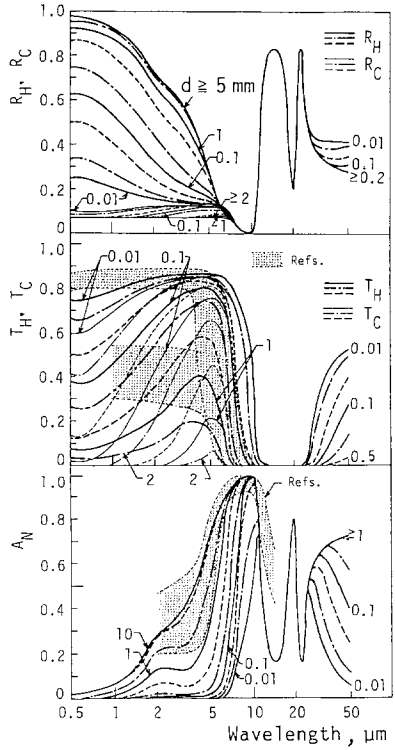

Fig. 5. Spectra of reflectance, transmittance, and absorptance of alumina ceramic layers.

figure, the determined value of K_e can be different by as much as 300% at maximum, depending on the blind choice of the phase function. But provided we never change the chosen assumption of the phase function in our evaluation of T_H or R_H of other systems of different τ, e.g., for the system of $\tau = 20\tau^0$, the errors in the evaluated values of T_H or R_H are of the order of 5%. The errors are not so serious as compared with the errors introduced by the gray approximation. It should be noticed that a crude model can make a good prediction of radiation transfer but that the property values obtained with the assumption of a model should be used with the model.

Figure 5 shows the radiation characteristics of an alumina ceramic layer [17], where A_N is the absorptance for the normal incidence and d is the thickness of the layer. The experimental values were analyzed using a four-flux model. The spectra of the property values were obtained and correlated for the systematic calculation of the macroscopic values for engineering applications.

5. HUMAN BODY AND ENVIRONMENTAL SURFACES FOR HUMAN LIFE

There is an increasing demand for radiation characteristics of human body and environmental surfaces for human life, relating to medical techniques, air-conditioning, designs of closing, architectual designs, and designs of city areas. The materials of interest are generally the media which scatter radiation in and/or at the surfaces of the materials. A simple and reliable technique for the measurement had not been established for these complex materials. Terada et al. [20] developed an ellipsoidal mirror technique to measure the spectra of scattering and absorption coefficients of a living human body. Yoshida et al. [21] developed an integrating sphere technique measuring hemispherical reflectance R_h for the hemispherical sky irradiation. Figures 6a and b show the schematic diagram of the measuring system and the measured spectra of a rice field, respectively. The notation h in Figure 6b is the solar height.

6. RADIATION PYROMETRY

Radiation pyrometry is closely related to the radiation characteristics of materials. Relating the solid materials used in the industry, the characterization of the surfaces is difficult, and the surface conditions may change continuously. Accordingly, it is preferable to measure the radiation characteristics such as the emittance simultaneously with the temperature. As for this idea, there have been two-color pyrometry and spectral (multi-

wavelength) pyrometry which measures emission of radiation at more than two wavelengths.

We presented the algorithm of multi-wavelength pyrometry measuring emission and reflection simultaneously and remotely [22]. In this method, the angular characteristics of reflection are considered properly to exclude the crude application of the Kirchhoff's law. The wavelength dependence of the angular characteristics of reflection is described by a simple expansion form in wavelength, while the emittance spectrum has been described by a simple expansion form in wavelength in the convensional techniques. Also, our method measures a larger number of quantities than are necessary for the analytical solution, and a least-squares method is applied. We developed a three-wavelength pyrometer on the basis of the above algorithm. It measures emission and reflection data at the three wavelengths. Experiments were performed on a specular-finished metal surface in an

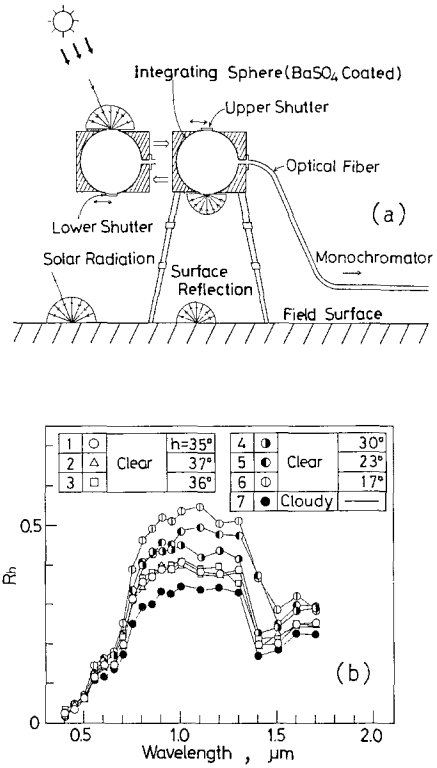

Fig. 6. (a) Measuring system for hemispherical reflectance of environmental surfaces; (b) reflectance spectra of a rice field.

oxidation process, where the radiation characteristics change drastically. Figure 7 shows an example of the results. The figure shows the temperature T^{tc} measured by a thermocouple. The measured emission quantities are shown in the form of emittance ε^{tc} calculated by using T^{tc}. The measured reflection quantities are shown in the form of R^*_{NN}. defined in Section 3. The temperature determined by the analysis is T^{opt}. The method is effective for non-transparent materials in isolated systems. Application of an infrared detector may be a possible choice for semi-transparent materials. The problem of the environmental irradiation has remained the greatest problem.

7. DEMAND FOR RADIATION DATA

Besides the demand mentioned in Section 5, there is strong demand for thermal radiation data in the fields relating to new materials and new production/measuring techniques. Of a number of materials or conditions, the demand for the optical constants of semi-conductors in the molten state and/or at high temperatures is very great. Infrared properties of molten salts [23] are also becoming important for the evaluation of radiation transmission in heat transfer materials and for the evaluation of radiation effects in thermophysical property measurements. There is also a strong demand for the characteristics of food.

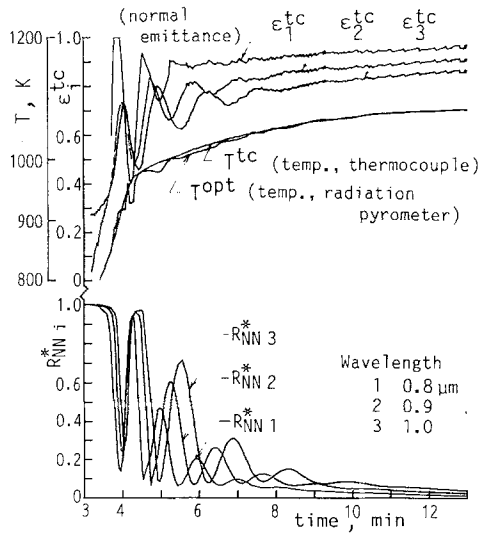

Fig. 7. Measured quantities and determined temperature by a pyrometer.

8. CONCLUSION

The development of engineering models is required for the systematic research of the complicated radiation phenomena. Further accumulation of data is also necessary. Additionally, new concepts are required for processing of the large number of measured data and collected information.

REFERENCES

1. T. Makino, *Netsu Bussei* **1**:68 (1987).
2. S. Roberts, *Phys. Rev. Ser. 2* **114**:104 (1959).
3. T. Makino and T. Kunitomo, *Bull. JSME* **20**:1607 (1977).
4. T. Makino, R. Kishida, H. Kawasaki, and T. Kunitomo, *Bull. JSME* **23**:1835 (1980).
5. T. Makino, T. Kunitomo, and T. Mori, *Bull. JSME* **27**:57 (1984).
6. T. Makino, H. Kawasaki, and T. Kunitomo, *Bull. JSME* **25**:804 (1982).
7. T. Makino, H. Kinoshita, Y. Kobayashi, and T. Kunitomo, in *Heat Transfer Science and Technology*, B. X. Wang, ed. (Hemisphere, Washington, D.C., 1987), pp. 756–763.
8. T. Makino, T. Kunitomo, H. Hasegawa, Y. Narumiya, and S. Matsuda, *Heat Transf. Jpn. Res.* **14**:16 (1985).
9. Y. S. Touloukian and D. P. DeWitt, eds., *Thermophysical Properties of Matter, Vol. 7* (IFI/Plenum, New York, 1970).
10. T. Makino, S. Matsuda, N. Hirata, and T. Kunitomo, in *Heat Transfer 1986, Vol. 2*, C. L. Tien, V. P. Carey, and J. K. Ferrell, eds. (Hemisphere, Washington, D.C., 1986), pp. 577–582.
11. T. Makino, *Proc. 7th Jpn. Symp. Thermophys. Prop.* (1986), p. 37.
12. T. Makino, O. Sotokawa, and Y. Iwata, *Int. J. Thermophys.* **9**:1121 (1988).
13. T. Makino and O. Sotokawa, *Proc. 25th Natl. Heat Transf. Symp. Jpn.* **2**:361 (1988).
14. T. Makino, T. Niwa, and T. Kasai, *Proc. 8th Jpn. Symp. Thermophys. Prop.* (1987), p. 101.
15. N. Matsumura, H. Izuma, S. Tsujimoto, and T. Kunitomo, *Proc. 1st Asian Thermophys. Prop. Conf., Beijing* (1986), p. 117.
16. H. M. Shafey, Y. Tsuboi, M. Fujita, T. Makino, and T. Kunitomo, *AIAA J.* **20**:1747 (1982).
17. T. Makino, T. Kunitomo, I. Sakai, and H. Kinoshita, *Heat Transf. Jpn. Res.* **13**:33 (1984).
18. H. S. Sang, A. Yoshida, and T. Kunitomo, *Proc. 1st Asian Thermophys. Prop. Conf., Beijing* (1986), p. 237.
19. T. Makino, M. Maerefat, and T. Kunitomo, in *Solar Energy Engineering 1987, Vol. 1*, Y. Goswami, K. Watanabe, and H. M. Healey, eds. (ASME, New York, 1987), pp. 172–177.
20. N. Terada, K. Ohnishi, M. Kobayashi, and T. Kunitomo, T., *Int. J. Thermophys.* **7**:1101 (1986).
21. A. Yoshida, S. Idei, K. Tominaga, and T. Kunitomo, *Heat Transf. Jpn. Res.* **18**:93 (1989).
22. T. Makino, T. Kosaka, J. Arima, S. Aoyama, and H. Tsujimura, *Trans. Soc. Instrum. Control Eng.* **24**:331 (1988).
23. T. Makino, T. Maeda, M. Edamura, and A. Yoshida, *Proc. 9th Jpn. Symp. Thermophys. Prop.* (1988), p. 119.